Correlation of seismotectonic variables and GPS strain measurements in western Turkey

Ali Osman Öncel
Active Fault Research Center, Geological Survey of Japan, Tsukuba, Japan

Tom Wilson
Department of Geology and Geography, West Virginia University, Morgantown, West Virginia, USA

Received 21 March 2004; revised 8 August 2004; accepted 27 August 2004; published 13 November 2004.

[1] Interrelationships between the multifractal properties of epicenter distribution (D_q), the Gutenberg-Richter b value, and GPS-derived strain (shear and dilatation) for the time period extending from 1981 to 1998 are examined in the eastern Mediterranean and western Turkey area. This analysis was conducted in three tectonic subdivisions corresponding to regions dominated by shear, extensional, and compressional deformation. The region of shear coincides with the Northern Anatolian Fault Zone (NAFZ); the region of extension, with the Aegean back arc region; and the region of compression, to the Aegean subduction zone between the African and Anatolian plates. The median b value in the region of extension is larger than those observed in the regions of shear and compression and suggests that large magnitude earthquakes are less probable in this region than along the NAFZ and Aegean subduction zone. A significant correlation is observed between D_2 and D_{15} with dilatation over the 10–40 km range in the back arc region of extension. A marginal correlation between GPS-derived strain and b value is observed only in the region of compression where it correlates negatively with shear and positively with dilatation. A significant positive correlation is observed between D and b along the NAFZ. A clear relationship between D and b does not exist in regions deformed by extension and compression. The relationship between D and b along the NAFZ may also be an indicator of increased seismic hazard since the positive relationship between D and b is a recent characteristic of the NAFZ observed only in the 20-year period preceding the Izmit earthquake. *INDEX TERMS:* 7215 Seismology: Earthquake parameters; 7209 Seismology: Earthquake dynamics and mechanics; 7223 Seismology: Seismic hazard assessment and prediction; 7230 Seismology: Seismicity and seismotectonics; *KEYWORDS:* GPS strain, fractal dimension, b value

Citation: Öncel, A. O., and T. Wilson (2004), Correlation of seismotectonic variables and GPS strain measurements in western Turkey, *J. Geophys. Res.*, *109*, B11306, doi:10.1029/2004JB003101.

1. Introduction

[2] Fractal analysis is often used to quantify the size-scaling attributes and clustering properties of seismotectonic variables. In recent years, fractal concepts have been widely used to characterize various aspects of landscapes, coastlines, rock fracture patterns, and seismicity and regional tectonics [*Nakaya and Hashimoto*, 2002; *Öncel and Wilson*, 2002; *Sunmonu et al.*, 2001]. It has been shown, for example, that earthquake magnitude and fault trace patterns have a power law distribution, which is often expressed by various estimates of their fractal dimension. These estimates include the capacity dimension (D_O) derived from box counting, the correlation dimension (D_C) of epicentral clustering derived from the two-point correlation function, and the Gutenberg-Richter b value derived from the slope of the earthquake frequency-magnitude relationship. Recent studies suggest that interrelationships between these complex variables, particularly the seismic b value versus the fractal dimension of epicenters (D_C) and capacity dimension of fault trace distribution (D_O), vary in a systematic way related to the earthquake process and fault complexity [*Öncel et al.*, 1995, 1996a; *Öncel and Wilson*, 2002; *Öncel et al.*, 2001]. For example, temporal variations between b value and the fractal dimension of hypocenters (D_C) tend to be negatively correlated over long time intervals. Changes in this correlation from negative to positive were observed along the Northern Anatolian Fault Zone (NAFZ) during the 25 year period preceding the 1999 Izmit earthquake [*Öncel et al.*, 1995; *Öncel and Wilson*, 2003]. Spatial variations of b and D_C are also negatively correlated along the NAFZ [*Öncel et al.*, 1996a]. Decreases of b in the

0148-0227/04/2004JB003101$09.00

central segment of the NAFZ are accompanied by increases of D_C.

[3] *Öncel et al.* [2001] also examined the spatial correlation of b value and the capacity dimension (D_O) for the active fault patterns throughout Honshu, Japan, and found patterns of both positive and negative correlation. Regions of positive correlation were interpreted to be regions in which stress was released through increased levels of low-magnitude seismicity along smaller fault strands. Regions of negative correlation were interpreted to be tectonic regions in which tectonic stress tended to be released through larger magnitude seismicity along larger interconnected fault strands.

[4] Multifractals provide a more complete characterization of both the spatial and the temporal properties of seismicity distribution than do monofractals [*Kagan*, 1994], since multifractal components provide additional information about the irregularities and complex dynamics of seismotectonic processes. In the following analysis of epicenter distributions, D_2 is interpreted to characterize regional-scale clustering while D_{15} is interpreted to characterize local-scale clustering in the region [*Godano and Caruso*, 1995]. For example, *Kagan and Jackson* [1991] evaluated temporal variation of multifractal characteristics for global seismicity of magnitude $M > 6.5$ from 1977 to 1988, and found a fractal dimension of 0.8–0.9. *Sunmonu et al.* [2001] also evaluated fractal properties of seismicity in the Himalayan region and obtained a fractal dimension of 0.95 for seismicity ($M > 7.0$) occurring during a 100 year period extending from 1895 to 1995.

[5] In this study, variations in the patterns of seismicity are considered for microearthquakes with magnitudes (M_D) ranging from 2.6 to 4.8 in addition to larger earthquakes with magnitudes (M_D) ranging from 4.6 to 6.0. Fractal analysis undertaken in this study is used to evaluate spatial changes in the fractal clustering of earthquake hypocenters in western Turkey where shallow and deep-seated seismicity appear to be concentrated near crustal faults associated with interaction between the subducting African plate and the overriding Aegean-Anatolian plate in the eastern Mediterranean [*Eyidogan*, 1988], along the transform boundary between the Anatolian and Eurasian plates in northern Turkey, and the region of extension between them.

2. Data

2.1. Seismicity

[6] A fairly uniform earthquake-monitoring network has been in operation in northwestern Turkey since 1970 [*Ucer et al.*, 1985]. Hence the station coverage since that time yields a reliable record of seismicity in all regions of the study area so that variations in the recorded patterns of seismicity are generally unrelated to variations in station coverage. In this study, the period of analysis is restricted to earthquakes occurring from 1981 to 1998. This observation period follows the upgrade of the Turkish and Greek Networks in 1980. The completeness of seismicity used in this study has been determined from frequency-magnitude (FM) statistics [*Wiemer and Wyss*, 2000]. Threshold magnitudes were determined from the goodness of fit to a fractal or power relation observed in the FM distribution. Limited station coverage can lead to reduced slope or anomalous slope breaks in the low-magnitude end of the FM plot. Since threshold limits are incorporated in the present study, slope changes resulting from inadequate station density are minimized. We used nearly half (31) of the 67 different seismic zones suggested by *Papazachos and Kiratzi* [1996] for western Turkey and the eastern Mediterranean. The region investigated in this study is confined to the area between 23°–31°E and 33°–43°N using seismicity data from the Kandilli Observatory and Research Institute (KOERI). (The data can be obtained directly from KOERI via ftp://ftp.koeri.boun.edu.tr/seismo/catalog/.)

[7] Robust fractal analysis requires a set of at least 100 events [*Havstad and Ehlers*, 1989]. This criterion was adopted since differences in fractal dimension with alpha levels less than 10% could not be found in data sets consisting of less than 100 events. Thus the analysis of seismicity patterns conducted here is restricted to the analysis of data sets including at least 100 events to insure that reliable estimates of fractal dimension are obtained. Under this restriction, there is insufficient data in several of the zones defined by *Papazachos and Kiratzi* [1996]. This is especially a problem in the eastern Mediterranean. To honor this restriction, some zones were combined into larger seismic zones to ensure that each zone contained at least 100 events. After these combinations were made, it was possible to subdivide the study area into a total of 25 seismic zones each of which contained 100 or more epicenters (Figure 1). Specifically, zones 9b–9c, 5b–5a–5A–5B, 4b–4B, and 4a–4A of *Papazachos and Kiratzi* [1996] were merged to form seismic zones 19, 23, 24, 25, respectively of our study. The completeness of the seismic record (or threshold magnitude) varies through the region from minimum magnitudes of 2.6 to 3.8 (see Table 1). This indicates that station coverage is not dense enough in some parts of the study area to record all events of $M_D \leq 2.6$. On the basis of the threshold analysis, minimum magnitudes as high as 3.8 (zone 23, Table 1) were used in this study.

[8] In addition, the analysis of seismicity conducted in this study was restricted to shallow events ($\leq$40 km) consistent with previous studies [*Papazachos and Kiratzi*, 1996]. The 40 km maximum depth was adopted in this study since, in general, the seismogenic layer is suggested to be only 20–30 km thick for western Turkey; however, on the basis of errors in hypocentral location, the less stringent lower limit of 40 km is adopted.

2.2. GPS-Derived Strain Rate Field

[9] GPS strains used in this study were taken from *Kahle et al.* [2000], covering the period of time extending from 1988 to 1998. The distribution of GPS control points used in this study is shown in Figure 1. The values of shear strain and dilatation computed from the GPS network are also shown in Figure 1. The 25 seismic zones into which the study area is subdivided are also outlined for reference. Kriging was used to interpolate the irregular distribution of observation points in the GPS network onto a regular 2.3 km (east-west) by 3.3 km (north-south) grid. Average shear strain and dilatation in each seismic zone were estimated by

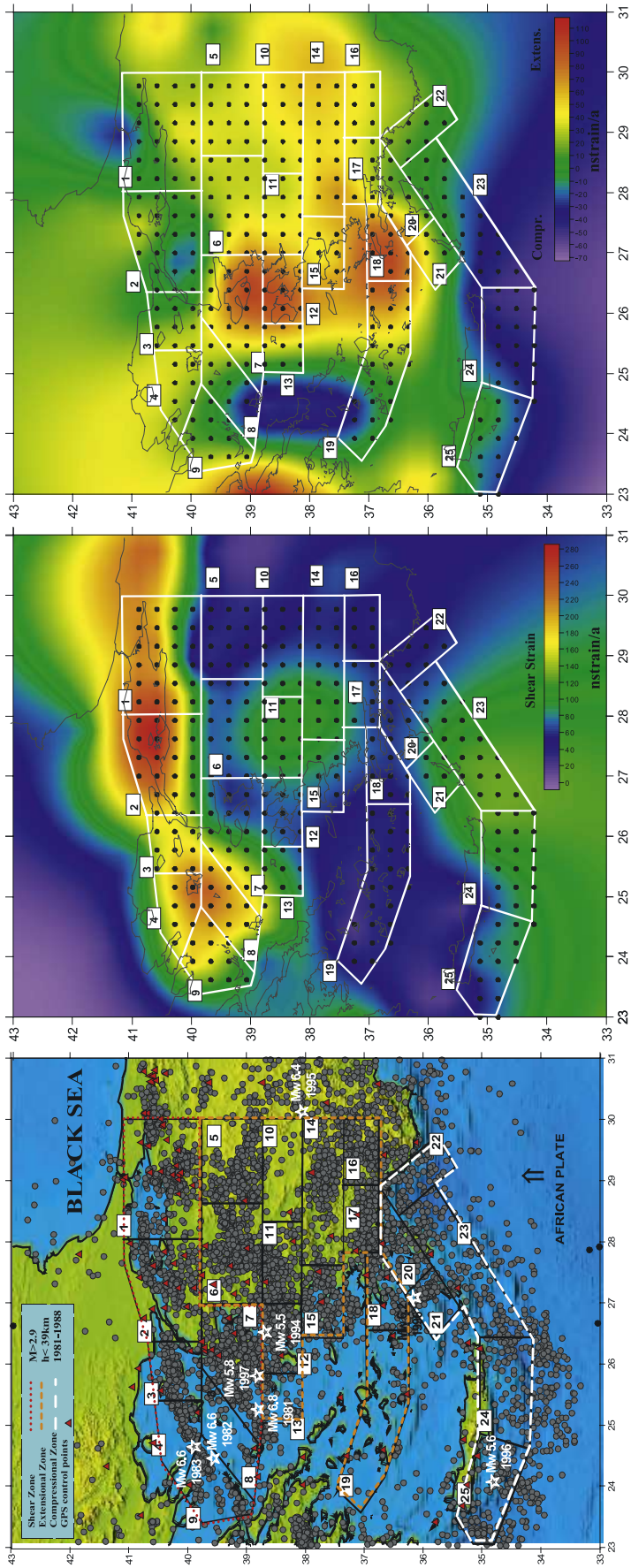

Figure 1. (right and middle) Contour maps of GPS-derived shear and dilatational strain, respectively. These contour maps were constructed using strain data presented by *Kahle et al.* [2000] for the eastern Mediterranean study area. Highlighted nodes were used to estimate the average strain within individual zones. (left) Map of the locations of GPS control points, events of M > 3.0 that occurred between 1981 and 1998, and the locations of the 25 seismic zones for which the analysis and comparisons presented in this paper were undertaken.

Table 1. Complex Variables (D and b Value), Average Shear and Dilatation, and Magnitude Range Used in the Study for Seismic Zones 1–25[a]

	Seismicity									
	Full		2–10 km		10–40 km				Strain, nstrain/yr	
A	D_2	D_{15}	D_2	D_{15}	D_2	D_{15}	b	M_L–M_U	Shear	Dilatation
					Strike Slip					
1	1.44	1.1	1.73	1.22	1.4	1.01	1.51	2.6–5.0	161.79	19.38
2	1.43	1.07	1.81	1.33	1.43	1.12	1.39	2.6–5.5	201.07	3.63
3	1.62	1.42	1.9	1.28	1.49	1.26	1.47	3.1–4.8	164.82	12.88
4	1.24	0.84	1.86	1.5	1.02	0.64	1.11	3.5–6.0	191.60	25.85
7	1.53	1.24	1.94	1.48	1.48	1.23	1.24	3.2–6.0	101.71	55.87
8	1.32	0.86	1.85	1.13	1.37	0.92	1.16	3.2–4.9	189.45	3.88
9	1.18	0.83	1.86	1.4	1.14	0.64	0.97	3.0–5.3	146.38	11.55
					Extension					
5	1.07	0.73	1.85	1.59	0.95	0.57	1.75	2.6–4.7	41.02	36.21
6	1.33	0.92	1.81	1.56	1.22	0.78	1.81	2.7–4.8	78.75	33.68
10	0.89	0.58	1.46	0.95	0.87	0.46	1.35	3.0–4.8	70.32	44.69
11	1.48	1.2	1.83	1.37	1.53	1.24	1.39	3.0–5.8	102.35	40.96
12	1.52	1.26	1.89	1.37	1.53	1.39	1.5	3.2–5.1	72.75	75.83
13	1.36	1	1.86	1.71	0.75	0.41	1.1	3.1–5.5	89.26	25.51
14	1.4	1.08	1.79	1.26	1.4	1.19	1.32	2.9–5.5	78.81	53.66
15	1.57	1.26	1.93	1.36	1.59	1.31	1.28	3.1–5.4	78.25	54.39
16	1.38	0.99	1.42	0.97	1.24	0.94	1.4	3.1–5.4	47.99	38.12
17	1.42	1.05	1.78	1.44	1.37	1	1.22	3.2–5.4	50.59	37.22
18	1.61	1.32	1.9	0.81	1.64	1.43	1.25	3.6–4.9	58.89	80.91
19	1.43	1.18	1.88	1.16	1.2	0.88	0.67	3.5–5.2	38.75	22.09
					Compression					
20	1.74	1.5	1.81	1.04	1.77	1.64	1.44	3.0–5.3	68.88	20.76
21	1.44	1.09	1.79	1.51	0.92	0.55	1.21	3.7–5.0	95.04	18.27
22	1.68	1.38	1.87	1.12	1.63	1.39	1.49	3.2–4.6	54.22	10.21
23	1.63	1.04	1.82	1.27	1.61	0.99	1.24	3.8–5.7	107.79	−22.87
24	1.65	1.23	1.57	0.93	1.75	1.47	1.08	3.7–5.5	103.39	−40.39
25	1.45	1.09	2	1.07	1.55	1.08	1.21	3.5–5.8	75.28	−16.12

[a] $D_2(10)$ refers to D_2 measured over the 2–10 km scale, etc. D_2 and D_{15} without parenthetical scale references were estimated over a full-scale range that varied from zone to zone but, on average, extended over the 10–80 km scale range. M_L is lower magnitude of completeness; M_U is upper limit of seismicity.

averaging the kriged estimates in each zone. Average values of shear and dilatation strain are listed in Table 1 for each seismic zone.

3. Data Analysis Procedures

3.1. Seismic b Value

[10] Estimates of b value in the *Gutenberg and Richter* [1954] relation

$$\log N = a - bM \tag{1}$$

imply a fractal relation between frequency of occurrence and the radiated energy, seismic moment, or fault length, and this is one of the most widely used statistical parameters to describe the size scaling properties of seismicity. The maximum likelihood method provides the least biased estimate of b value [*Aki*, 1965]:

$$b = 2.303/(M_{mean} - M_{min} + 0.05) \tag{2}$$

where M_{mean} is the mean magnitude of events and M_{min} is the minimum magnitude of completeness in the earthquake catalogue. Accurate estimates of local changes of M_{min} can be made if relatively large numbers (100 or so) of local observations are available for analysis [*Wiemer and Wyss*, 2000]. Seismic b value is negatively correlated to mean magnitude and mean crack length [*Main*, 1996]. The value 0.05 in equation (2) is a correction constant that compensates for round off errors. The 95% confidence limits on the estimates of b are $\pm 1.96b/\sqrt{n}$, where n is the number of earthquakes used to make the estimate. This yields confidence limits on b value of ±0.1–0.2 for a typical sample consisting of n = 100 earthquakes.

3.2. Generalized Fractal Dimension D_q

[11] Earthquake magnitudes and hypocenter distribution are examples of complex natural phenomena that have scale-invariant structure. The evolution of ideas concerning the fractal characterization of natural phenomena has been expanded to incorporate multiple measures of fractal dimension or scaling exponent. Further explanation of the fractal character of seismological data requires more than one fractal dimension. *Kagan* [1994], for example, suggests that a single fractal dimension does not adequately describe geometrical irregularities since two objects with the same fractal dimension could have significantly different properties and most geodynamical processes have geometrical interrelationships that vary with scale. Multifractals are used

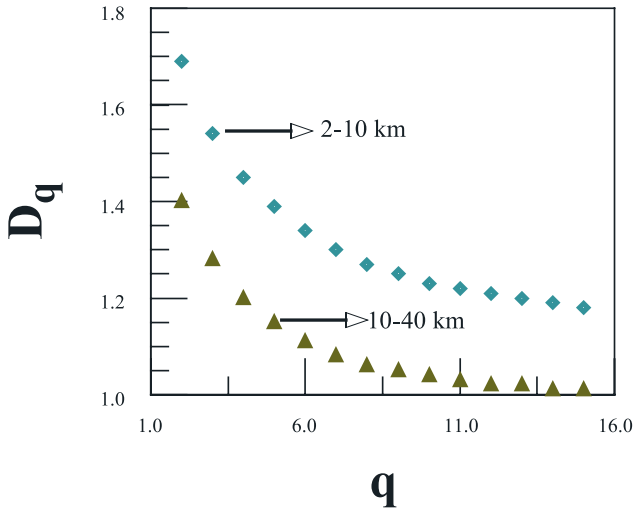

Figure 2. Spectrum of D_q versus q for seismic zone 1.

to describe a heterogeneous fractal set. Following *Grassberger and Procaccia* [1983] and *Hentschel and Procaccia* [1983], the generalized dimension (D_q) is defined as

$$D_q = \frac{1}{(q-1)} \lim_{l \to 0} \frac{\log \sum_{i \in l} p_i^q}{\log l} \tag{3}$$

where p_i is the probability that a box of size l will contain part of the pattern (or, in the present context, one or more epicenters). The standard error in the estimate of D is, on average, ±0.03, and ranges from approximately ±0.01 to ±0.05. The discrete form of the generalized correlation integral function [*Hirabayashi et al.*, 1992] is defined as

$$C_q(r) = \frac{1}{N} \left[\sum_{j=1}^{N} \left(\frac{N_j(R \le r)}{N-1} \right)^{q-1} \right]^{1/(q-1)} \tag{4}$$

[12] The spectrum of the generalized fractal dimensions (D_q, q = 0, 1, 2,...) of hypocenter distributions estimated from the linear portion of the log-log plot of C_q versus distance can be used to evaluate the distribution for multifractal behavior. The better known capacity, information, and correlation dimensions correspond to values of q = 0, 1, and 2, respectively. The differences between heterogeneous and homogeneous fractals are inferred from variations in D_q. It is the variability of D_q that identifies multifractal behavior. In contrast, a monofractal is characterized by invariant D_q and is associated with relatively homogeneous geometry at all scales. Multifractal exponents can be computed for both positive and negative values of q, and are interpreted to characterize the degree of clustering from highly to sparsely clustered, respectively. Our study is restricted to computation and analysis of fractal dimensions with positive q values of 2 and 15. The variation of D_q versus q for seismic zone 1 (Figure 2) reveals consistent decreases in D as q increases from 2 to 15 and D_2 is always greater than D_{15}. Values of q greater than 15 were not computed in the present study since the results of *Lei et al.* [2003] showed that D does not change significantly when q is greater than 15.

[13] The log(r) versus log (C_r) plots of multifractal components D_2 through D_{15} are shown for selected seismic zones through the study area in Figure 3 and the time variation of seismicity in those zones is illustrated in Figure 4. D_2, the correlation dimension, is sensitive to small changes in the density of points within small subdivisions of the pattern. The higher-order dimensions are increasingly sensitive to heterogeneity in the distribution of points. Since D_{15} is usually less than D_2, this suggests that seismicity is more clustered at local scales.

3.3. Statistical Comparison

[14] In the following analysis we evaluate the statistical significance of differences in median value using the Mann-Whitney test [*Davis*, 2002]. The Mann-Whitney test is a nonparametric alternative to the t test that does not require that observations come from normally distributed parent populations. The Kolmogorov-Smirnov test was first used to determine whether sample observations were normally distributed. In the majority of cases, the observations of b value, D, magnitude, and strain are not normally distributed and so the nonparametric Mann-Whitney test was used instead of the t test.

[15] In the Mann-Whitney test, the two samples are combined and ranked. The test is based on differences in the sum of the ranks for the two samples. A given difference in the sum of the ranks will have some probability of random occurrence for samples drawn from the same parent population. Large differences in the sum of ranks have lower probability of occurrence than smaller differences. Just as with the t test, the probability or risk you are willing to accept as a criterion for significance in the difference is referred to as the α level. In the majority of cases we will specifically cite the probability p that the two samples could be drawn at random from parent populations that have equal median.

[16] In practice, the difference in median value is considered statistically significant if the probability (p) that they are identical is less than 0.05. This threshold probability is referred to as the α level. Conclusions about differences of median value can be stated as one- or two-tailed results. That is, it is possible to conclude that the median of one sample is greater than the median of another sample (a one-tailed test) or, simply, that the means are different (a two-tailed test). In the following discussions, if the median value of a statistic in one area is referred to as greater than that in another area, then the test is a one-tailed test. The one-tailed probability is half the two-tailed probability.

[17] The following statistical comparisons also include regression analysis conducted to determine whether linear relationships exist between seismotectonic variables. The regression analysis yields a correlation coefficient which is a measure of how well the variations associated with one variable predict those associated with another variable. The significance of the correlation coefficient is evaluated by computing the probability that the slope of the regression line could actually be zero. The significance of the regression coefficients (i.e., the slope and intercept) can be estimated using a t test [see *Davis*, 2002]. In this case the t statistic is estimated from the variance of the slope about

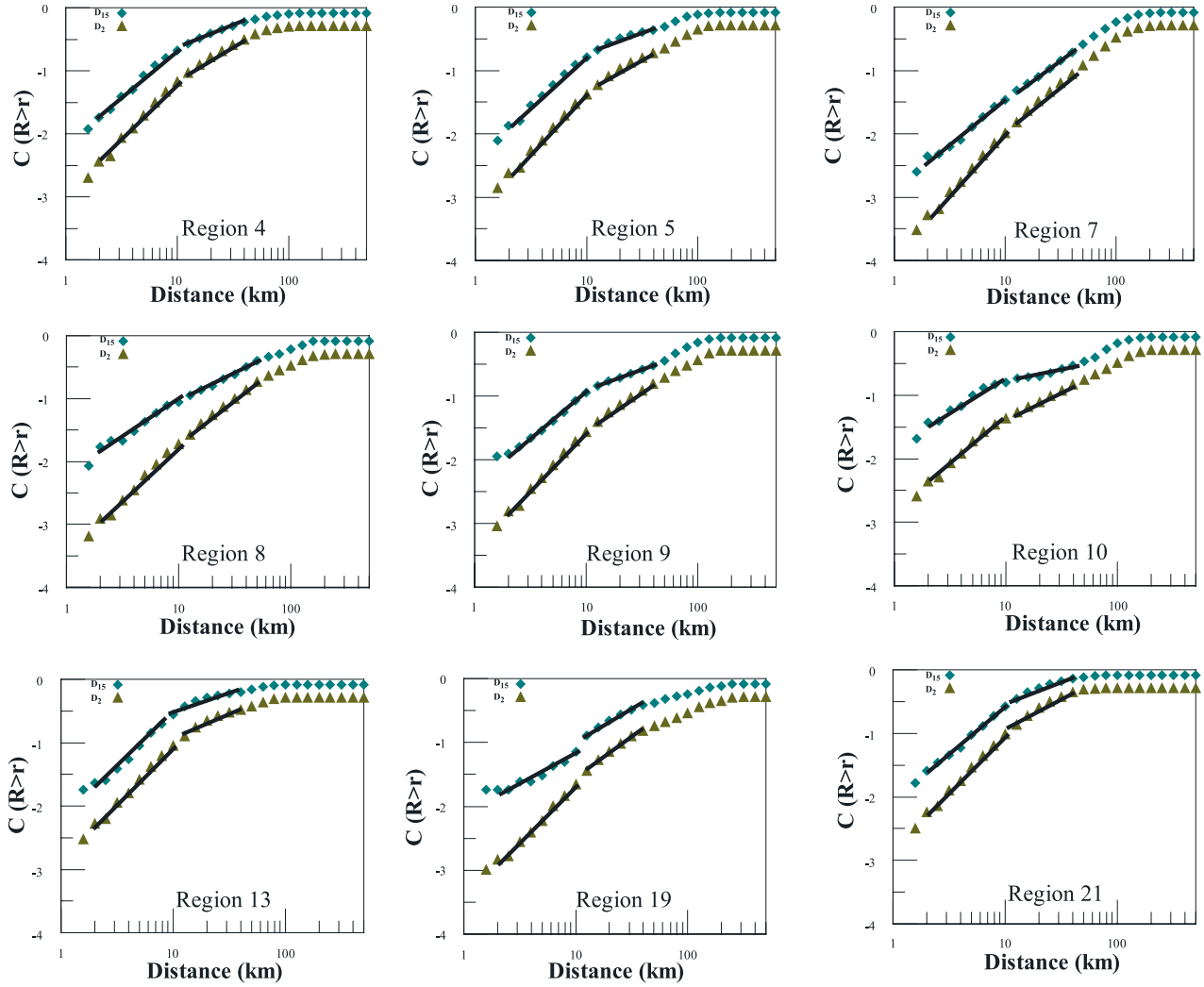

Figure 3. Generalized correlation integral functions derived from epicenter distributions in seismic zones 4, 5, 7, 8, 9, 10, 13, 19, and 21. Regression lines fit to the 2 to 10 and 10 to 40 km intervals are shown. Fractal plots for q varying from 2 to 15 are identified by different symbols.

the regression line. In our analysis we present correlation coefficients for relationships between seismotectonic variables, and note the probability, p, that the slope of the regression line could be zero. The test statistic is derived from the confidence interval about the regression line and thus is a two-sided test. In general, we state the probability that the correlation coefficient could actually be zero or have opposite sign. We use a cutoff probability or α level of 0.05 unless otherwise stated. Thus, for a correlation coefficient $r = 0.7$ and $p = 0.03$, there is a 0.03 probability that the population parameter (actual slope, for example) could be zero. We consider the correlation to be significant since $p \leq \alpha$.

4. Results

4.1. Scale Transitions in the Patterns of Earthquake Seismicity

[18] Fractal analysis of scaling relationships observed in patterns of seismicity and fracture systems often reveal the presence of scale transitions [*Main*, 2000; *Wilson*, 2001]. In this study we also examine the log(r) versus log (C_r) plots for changes of slope with scale (r). Regression lines calculated for the 2 to 10 km and 10 to 40 km subdivisions of the log (r) versus log (C_r) plots are shown for several seismic zones within the study area (Figure 3). Transitions were not observed in all seismic zones, and they do not always occur at the same value of *r*. Examination of all log(r) versus log (C_r) plots generally revealed slope transitions in the 5 to 20 km range. For this study we chose to compare variations of D over the 2 to 10 km and 10 to 40 km range to determine if systematic differences exist in the behavior of the log(r) versus log (C_r) plots (see Table 2). Values of D derived over the 2 to 10 and 10 to 40 km scales as well as full range estimates are compared to b value and GPS strain (shear and dilatation strains) in Table 3.

[19] Previous research suggests that slope breaks observed in the fractal analysis of seismicity distributions may be associated with the thickness of the seismogenic zone or with changes in cluster size [*Öncel et al.*, 1995, 1996a, 1996b]. *Öncel et al.* [1995] make this interpretation for slope breaks observed along the western length of the Northern Anatolian Fault Zone. *Pacheco et al.* [1992] report similar interpretations for earthquake data. *Öncel et al.*

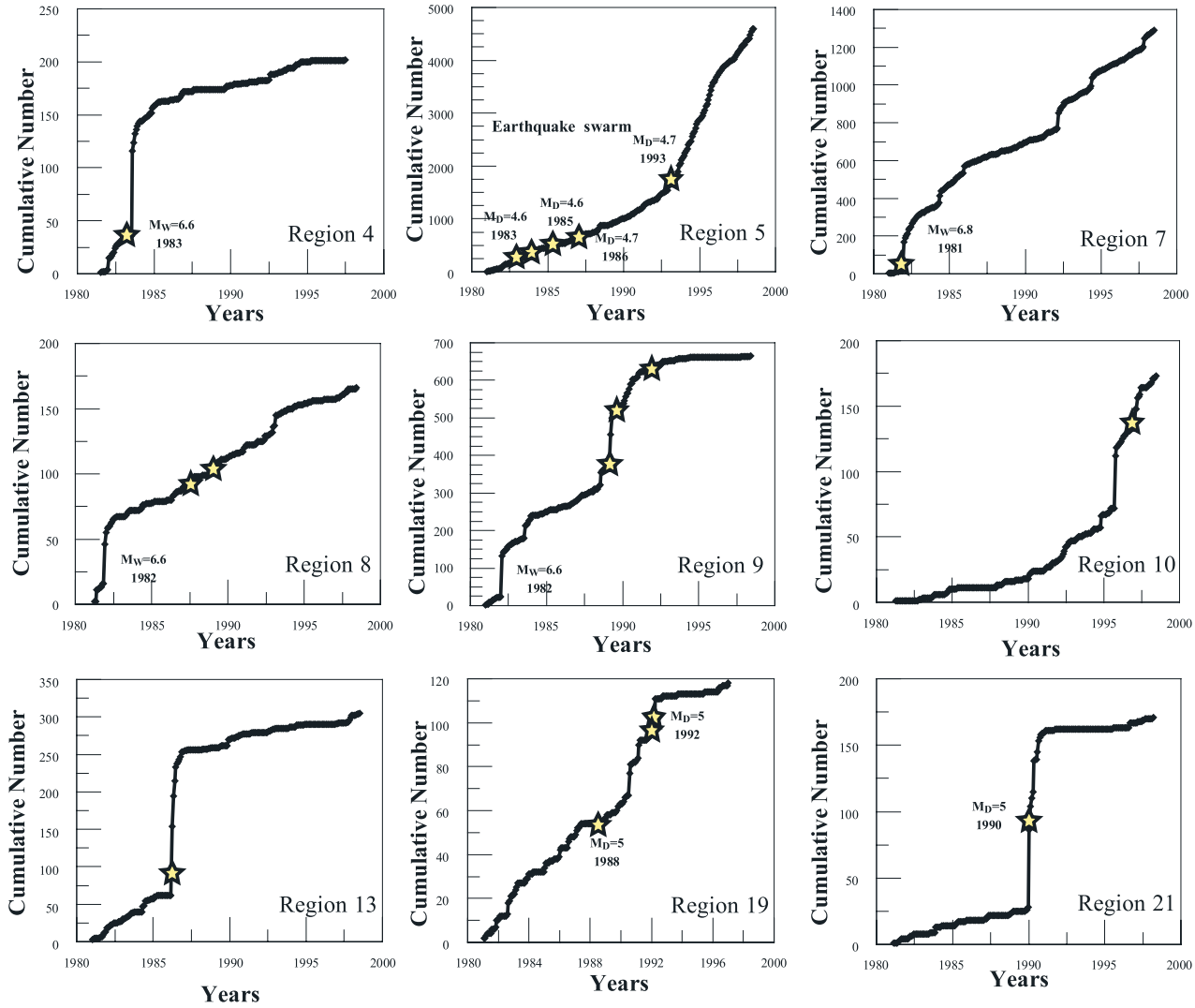

Figure 4. Time variations in the seismicity rate for the zones in Figure 3.

[1996a] found that for scales less than 20 km the fractal dimension ($D_{<20}$) was greater than that ($D_{>20}$) observed for scales greater than 20 km. Previous analysis conducted in several subdivisions of the NAFZ found the following relationship between $D_{<20}$ and $D_{>20}$: 1.98 and 1.36, respectively, in the central NAFZ; 1.85 and 1.28, in region 2; 1.99 and 1.15, in region 3; 2.12 and 1.38, in region 4; and 1.77 and 1.22, in region 5 [see *Öncel et al.*, 1996a, Figures 7 and 9]. The results reveal a consistent relationship between the fractal dimension observed at scales less than 20 km and

Table 2. Median/Mean Values of Multifractal Correlation Dimensions D_2 and D_{15} for the Full Range, 2–10 km Range and 10–40 km Range for Each Tectonic Subdivision of the Study Area (Shear, Extension, and Compression)[a]

	Full Range	2–10 km	10–40 km	b	Shear	Dilatation
			Shear			
D_2	1.43/1.39	1.86/1.85	1.4/1.33	1.24/1.26	164.8/165.3	12.88/19
D_{15}	1.07/1.05	1.33/1.33	1.01/0.97			
			Extension			
D_2	1.41/1.37	1.84/1.78	1.3/1.27	1.34/1.34	71.54/67.3	39.5/45.3
D_{15}	1.06/1.05	1.36/1.29	0.97/0.97			
			Compression			
D_2	1.64/1.6	1.82/1.81	1.62/1.54	1.23/1.28	85.16/84.1	−3/−5
D_{15}	1.16/1.22	1.1/1.16	1.24/1.19			

[a]The median/mean values of b, shear, and dilatation are also listed for each tectonic region.

Table 3. Correlation Coefficients for Comparisons Between the Complex Seismotectonic Variables D_2, D_{15}, and b, and GPS-Derived Shear and Dilatation Strain Rates Along the Northern Anatolian Fault Zone, the Aegean Back-Arc Region (Region of Extension), and the Aegean Subduction Zone (a Region Deformed Largely Under Compression)[a]

	Full Range					2–10 km Range					10–40 km Range				
	D_2	D_{15}	b	Shear	Dilation	D_2	D_{15}	b	Shear	Dilation	D_2	D_{15}	b	Shear	Dilation
Region of Strike Slip[b]															
D_2		0.97	0.81	−0.29	0.28		0.50	−0.39	−0.49	0.49		0.96	0.74	−0.26	0.08
D_{15}	(0)		0.75	−0.38	0.31	(0.25)		−0.40	−0.39	0.65	(0.00)		0.77	−0.28	0.23
b	(0.03)	(0.05)		−0.1	−0.06	(0.39)	(0.37)		−0.10	−0.06	(0.06)	(0.05)		−0.10	−0.06
Shear	(0.52)	(0.4)	(0.83)		−0.79	(0.26)	(0.39)	(0.83)		−0.79	(0.57)	(0.54)	(0.83)		−0.79
Dilation	(0.55)	(0.5)	(0.9)	(0.03)		(0.26)	(0.12)	(0.90)	(0.03)		(0.86)	(0.63)	(0.90)	(0.03)	
Region of Extension[c]															
D_2		0.98	−0.29	0.18	0.40		0.48	−0.13	0.18	0.20		0.98	0.00	0.13	0.67
D_{15}	0		−0.38	0.18	0.46	(0.12)		0.28	0.31	−0.44	(0.00)		−0.05	0.15	0.73
b	(0.36)	(0.23)		0.18	0.21	(0.69)	(0.38)		0.18	0.21	(0.99)	(0.88)		0.18	0.21
Shear	(0.57)	(0.59)	(0.57)		0.13	(0.57)	(0.34)	(0.57)		0.13	(0.68)	(0.65)	(0.57)		0.13
Dilation	(0.19)	(0.13)	(0.51)	(0.67)		(0.54)	(0.15)	(0.51)	(0.67)		(0.02)	(0.01)	(0.51)	(0.67)	
Region of Compression[d]															
D_2		0.76	0.51	−0.25	0.03		0.21	0.44	−0.54	0.38		0.90	0.22	−0.22	−0.41
D_{15}	(0.08)		0.71	−0.68	0.47	(0.69)		−0.02	0.26	0.46	(0.01)		0.39	−0.44	−0.10
b	(0.30)	(0.12)		−0.83	0.73	(0.38)	(0.97)		−0.83	0.73	(0.68)	(0.45)		−0.83	0.73
Shear	(0.64)	(0.14)	(0.04)		−0.6	(0.26)	(0.62)	(0.04)		−0.60	(0.68)	(0.39)	(0.04)		−0.60
Dilation	(0.96)	(0.34)	(0.10)	(0.21)		(0.46)	(0.37)	(0.10)	(0.21)		(0.43)	(0.84)	(0.10)	(0.21)	

[a]Values in parentheses indicate the probabilities (p) that these correlations are actually zero or could occur at random.
[b]North Anatolian Fault Zone.
[c]Central Australia.
[d]Southwestern Anatolia.

that observed at scales greater than 20 km along the NAFZ; D derived from the local (r < 20 km) variability is considerably larger than D derived from regional-scale variability (r > 20 km). A detailed examination of the multifractal log(r) versus log (C_r) plot from seismic zone 13 (Figure 5) reveals scale transitions around 21 km. This scale transition is believed to be associated with presence of an aftershock sequence produced by the 25 March 1986

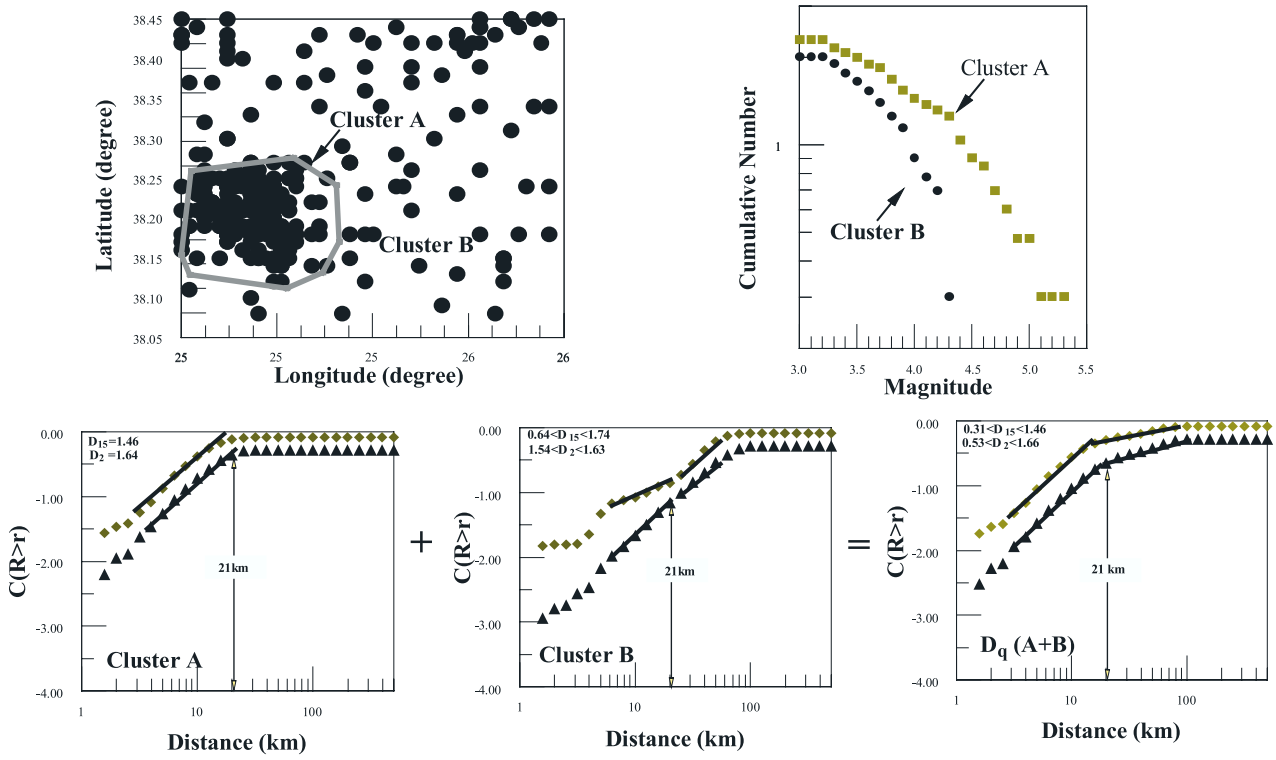

Figure 5. Seismicity in seismic zone 13. Three fractal and frequency-magnitude plots are presented; one for the entire zone, one for the area containing the aftershocks, and one for the area to the east of the area containing aftershocks. A distinct break in slope is observed in all three plots near r = 21 km.

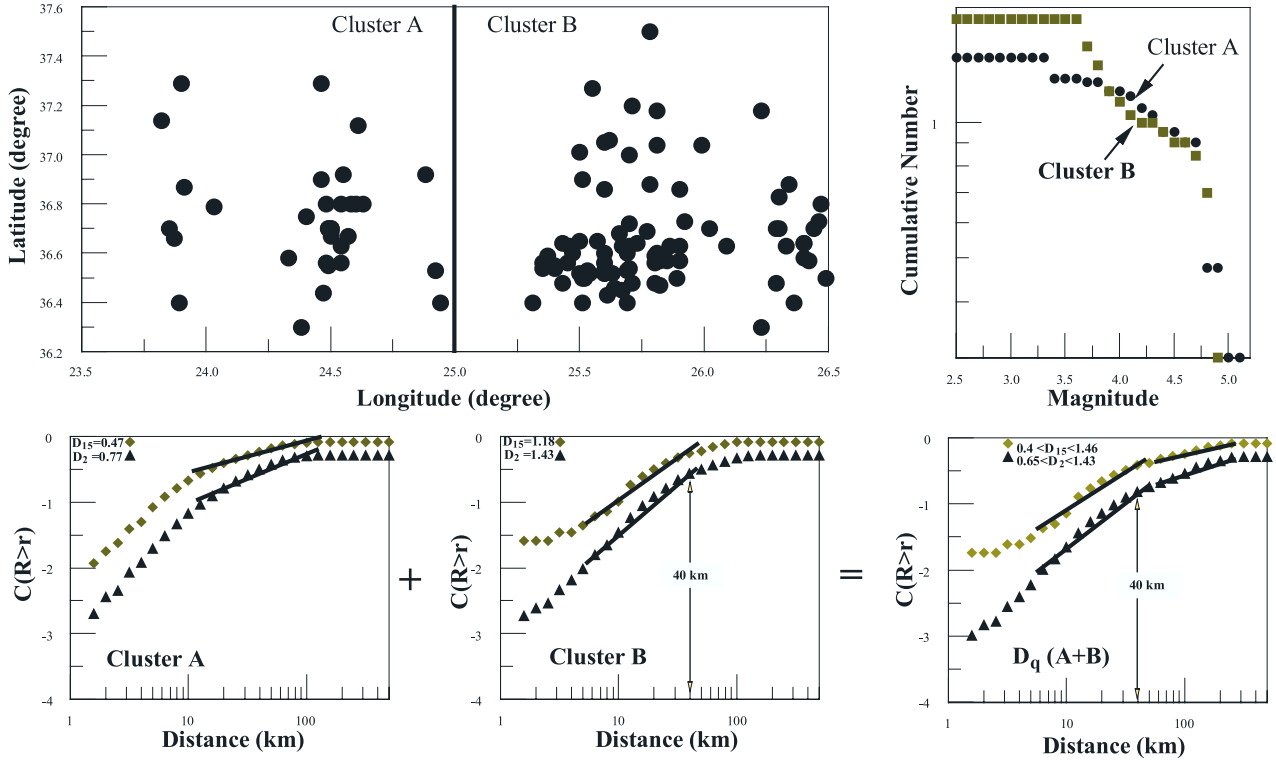

Figure 6. Seismicity pattern in seismic zone 9 and the fractal plots for the two subzones (clusters A and B).

(M = 5.2) earthquake in the region. In this case seismicity is concentrated in a nearly circular area approximately 16 km in diameter. D_2 and D_{15} measured at scales less than 21 km have value 1.16 and 1.46, respectively. At more regional scales (distances greater than 21 km), D_2 and D_{15} are 0.53 and 0.31, respectively. Dense clustering implied by the lower fractal dimension at more regional scale is interpreted to be an artifact of the aftershock activity and not really a long-term characteristic of that zone. The result also suggests that heterogeneity in the catalogue due to inclusion of secondary events (aftershocks) might be distinguished by scale changes in fractal distribution. The significance of these observations is explored further by dividing this seismic zone into two subregions consisting of the aftershock zone (cluster A) and the remainder of the seismicity outside the aftershock zone (cluster B) (see Figure 5). The log C(r) versus log (r) plot reveals distinct slope breaks at 21 and 3 km similar to those observed for the whole area. Slope breaks for seismicity outside the area directly affected by the aftershock sequence reveal additional variability in the background seismicity pattern. With the exception of q = 2, a distinct slope break occurs near r = 21 km. $D_{q=2}$ corresponds to the correlation dimension (D_C). Changes between the fractal dimension (D_C) and multifractal (q = 3–15) measures illustrate the sensitivity of multifractal characterization to changes in the local complexity. The location of the slope break at 21 km in both the aftershock zone (cluster A) and surrounding area (cluster B) suggest that the main event may have had some influence on stress distribution outside the immediate area affected by the aftershock sequence.

[20] In general, differences between D_2 and D_{15} are related to differences in the tendency for seismicity to be clustered or dispersed at different scales. However, the changes in D may also be associated with merging of events in border areas separating different tectonic regions. Seismic zone 19 (Figure 6, cluster A), for example, straddles the border between the region of extension (cluster A) and region of compression (cluster B). Seismicity associated with the extensional and compressional subdivisions in this zone were separated and analyzed independently. The multifractal spectra for the extensional and compressional subdivisions of this zone (Figure 6, cluster B) are characterized by D_q that are, on average, greater than or less than those derived for the zone as a whole. Fractal dimensions computed for seismicity in the extensional part of region 19 (cluster A) range from 0.76 (D_2) to 0.46 (D_{15}), and this suggests that seismicity is more densely clustered than in the compressional part (cluster B) where D ranges from 1.43 (D_2) to 1.18 (D_{15}). This suggests that mixing seismic events from different tectonic regions may lead to deviation in fractal distribution. The overlap, in this case, resulted from the necessity to combine smaller seismic zones into a single larger zone so that the number of events being analyzed would be at least 100. This number is generally required to accurately assess significance of differences between regions. In general, seismic zones lie in one tectonic subdivision or another and the effects noted here associated with overlapping source mechanisms are minor.

[21] Differences between the multifractal dimensions D_2 and D_{15} are interpreted to result from fractal heterogeneity between regional and local scales, respectively. In general, D and the paired differences in D are not normally distributed.

Thus the nonparametric Mann-Whitney test [*Davis*, 2002] was used to evaluate differences in median values of D_2 and D_{15} in each tectonic subdivision. At full scale, D_2 is greater than D_{15} in all three tectonic subdivisions. The probability that D_2 and D_{15} (full scale) are associated with populations having equal median is very low (generally < 0.01, two tailed). With one exception D_2 is significantly greater than D_{15} when measured over the 2 to 10 and 10 to 40 km scales at an α level = 0.025 (one-tailed). The differences are significant at all scales except for the difference between D_2 and D_{15} measured over the 10 to 40 km scale in the region of compression. In the region of compression, the probability (p) that the two median values are the same increases to 0.122 (one tailed probability of 0.06). Fractal heterogeneity ($D_2 - D_{15}$) measured for the different tectonic subdivisions of the study area over the full range of the log(r) versus log(C_r) plot (Table 2) is found to be 0.34 along the NAFZ transform zone, 0.32 in the divergent back arc region, and 0.38 along the subduction zone.

[22] The results presented in Table 2 also suggest that D_2 and D_{15} may differ between tectonic regions. For example, the median value of D_2 in the region of compression (1.64) is significantly higher than D_2 in the regions of shear and extension (1.43 and 1.41, respectively). The slight difference between D_2 observed in the regions of shear and extension is not significant. The significant difference in D_2 observed between the region of compression and the regions of extension and shear occurs only for the full-scale measurements (p = 0.01). No significant differences were observed in the median values of D_{15} over the full or restricted scale ranges. The difference in D_2 computed over the full range of scales suggests that seismicity is less clustered or more diffuse (higher D) in regions undergoing compressional deformation than in regions undergoing shear or extensional deformation. The degree of clustering in regions undergoing shear and extensional deformation are very similar. However, the median magnitude of earthquakes included in the analysis conducted in the region of compression (M3.6) is significantly larger than median values of earthquake magnitudes occurring in the regions of shear and extension (M3 and M3.1, respectively). Also note that the median b value in the region of compression (1.23) is smaller than the median b values observed in the regions of extension and shear (1.33 and 1.24, respectively). However, the nonparametric Mann-Whitney test suggests these differences are not significant. In addition, the lower b value in the region of compression could be due to the slightly higher average threshold magnitude used in that region.

[23] While the differences in D_2 between the region of compression and regions of extension and shear are significant over the full range, statistically significant differences are not observed over the 2 to 10 km and 10 to 40 km scales. However, the difference is closer to significant over the 10 to 40 km range than over the 2 to 10 km range. This suggests that the tendency toward increased clustering in regions of extension and shear is associated more so with behavior over the 10 to 40 km scale range.

4.2. Variations of Complex Variables in Western Anatolia

[24] Seismicity in western Turkey and the eastern Mediterranean is associated with a variety of tectonic features, focal mechanisms, evolution of stress and systematic differences in seismic moment [*Eyidogan*, 1988; *Taymaz et al.*, 1991]. The seismic zones mentioned earlier were grouped into regional subdivisions based on the predominant style of deformation occurring in those regions. These regional tectonic subdivisions are based on fault plane solutions for the period 1953–1999 [*Kiratzi*, 2002]. Correlations between the D_2, D_{15}, b, and GPS-derived strains are tabulated in Table 3. Table 3 also includes computed correlations over different scale ranges mentioned above, including: the full range that extends approximately from 2 to 80 km; the crustal scale, 10 to 40 km range; and the local or shallow, 2 to 10 km range.

4.2.1. Strike-Slip Tectonic Region (Northwest Anatolia)

[25] The tectonic subdivision including seismic zones 1, 2, 3, 4, 7, 8, and 9 (Figure 1) in northwest Turkey is associated with maximum dextral shear strain rates along the present-day Northern Anatolian Fault Zone (NAFZ) and its continuation into the northern Aegean Sea [*Kahle et al.*, 1998]. The temporal increase in seismicity rate from 1981 to 1988 is largely associated with aftershocks of larger earthquakes such as the 1981 (M_w = 6.8), 1982 (M_w = 6.6), 1983 (M_w = 6.6) in zones 4, 7, 8, 9 (see Figures 1 and 4). Seismicity in the remainder of this region is related to the interseismic deformation. Thus the regional seismicity in this area is related to postseismic and interseismic deformation. GPS strain data reveal both transpressional and transtensional stress behavior along the NAFZ, where the compressive stress orientation is NE-SW and extension occurs in NW-SE direction [*Kahle et al.*, 1999]. Correlation coefficients calculated between multifractal dimensions D_2 and D_{15} (measured over the full range) and b value (see Table 3) are positive (0.81 and 0.75, respectively) and significantly greater than 0 with p values of 0.03 and 0.05, respectively.

[26] The positive correlation between D and b over the full range and 10 to 40 km range suggests that an increased likelihood of low-magnitude seismicity is associated with increasingly dispersed (less clustered) epicenter distributions along the NAFZ strike-slip zone. The relationship appears to be associated primarily with deeper seismicity or larger crustal regions since correlation coefficients between D_2 and D_{15} over the 10 to 40 km scale with b are 0.74 and 0.77, respectively and the probability that the relationship could have zero slope is fairly low (0.06 and 0.05, respectively). Correlations of D_2 and D_{15} measured over the 2 to 10 km range with b value are not significant ($r_2 = -0.39$, with p = 0.39 and $r_{15} = -0.4$ with p = 0.37). In addition, no significant correlation is observed between D and b with shear or dilatation strain; however, shear strain does correlate negatively with dilatation strain in this region (−0.79 with a p value of 0.03).

4.2.2. Region of Extension Tectonics (Central Anatolia)

[27] A second tectonic subdivision characterized predominantly by extensional plate interactions is associated with seismic zones 5, 6, and 10–19 (Figure 1). This subdivision is located in the central part of Turkey and is characterized by a number of grabens bounded by high-angle normal faults. Two of the largest earthquakes observed in this area during the period of time examined in this study occurred in 1986 (seismic zone 13) and 1995 (seismic zone 10). The 1986 earthquake in zone 13 had a magnitude (M_S) of 5.6

and the earthquake in zone 10 had a magnitude (M_w) of 6.4. These earthquakes coincide with increases of seismic activity in zones 10 and 13 (see Figures 1 and 4). Seismicity in zone 5 has considerable variability in distribution due to the presence of an earthquake swarm in the area. The maximum magnitude of earthquakes in the swarm is M_D = 4.7 (see Figure 4).

[28] This extensional tectonic subdivision lies in the back arc region of the Aegean subduction zone [e.g., *Papazachos and Kiratzi*, 1996]. In this subdivision, D_2 and D_{15} correlate positively with dilatation over the 10–40 km range (r = 0.67 and 0.73 with p = 0.02 and 0.01 respectively). The correlations suggest that increased rates of extension produce increasingly dispersed seismicity. Significant correlation is not observed between D and dilatation over the full and 2 to 10 km scales. No correlation is observed between b value and strain or b value and D in this extensional subdivision.

4.2.3. Region of Compression (Southwestern Anatolia)

[29] Seismicity in the southwestern part of the study area is associated with a subduction zone. The region is dominated by thrust faulting, however, the eastern part of the zone includes a significant strike-slip component [*Taymaz et al.*, 1991]. This tectonic subdivision is located in subareas 20 through 25. Subduction in this region has been active since the Tertiary [*Dewey et al.*, 1973; *Main and Burton*, 1989; *Smith*, 1976]. Earthquake swarm activity in seismic zone 21 led to an increase in seismicity rate during 1990. The maximum magnitude of events in the swarm reached M_D = 5.0 (see Figure 4).

[30] Variations of b value correlate negatively with shear (r = −0.83, p = 0.04) in the zones of this subdivision. The correlation of b to dilatation is weakly positive (r = 0.73, p = 0.1). One would expect seismicity to correlate more so with dilatation in a subduction zone. However, dilatation along the subduction zone is on average only slightly negative. Dilatation is positive in the areas to the northeast (17 nstrain/yr) and negative (−29 nstrain/yr) farther west along the subduction zone. This combination of positive and negative dilatation along the subduction zone is probably responsible for the lack of a more significant correlation between b value and dilatation.

4.2.4. Relation Between Seismicity and GPS Strain

[31] Seismic activity in the western part of Turkey is controlled by different styles of tectonic deformation that include transform motion along the NAFZ in the north, extension within the western Anatolian graben complex such as the Gediz graben (regions 10–11) and the Menderes graben (regions 14–15) in the back arc area of the SE Aegean subduction zone, and compression along the subduction zone where the African Plate descends beneath the Aegean-Anatolian Plate [*Kahle et al.*, 2000]. Significant variation in shear and dilatation strain occurs throughout the study area (see Figure 1 and Table 1). Average shear strains in the shear, extension, and compressive tectonic regions are about 165.3, 67.3, and 84.1 nstrain/yr, respectively. The distribution of gridded values of shear and dilatation were in many instances not normally distributed; hence the nonparametric Mann-Whitney test [*Davis*, 2002] was used to evaluate the significance of differences in median value. The median values of shear strain in the shear, extension and compressive tectonic regions are 164.8, 71.5, and 85.2, respectively. Shear strains observed in the region of shear along the NAFZ are significantly greater than those observed in the regions of extension and compression (significant with α of 0.01). There is no difference between median shear strain observed in the regions of compression and extension. Average dilatational strain varies considerably through the study area as a whole. Average dilatation in the regions of shear and extension are 12.9 and 39.5 nstrain/yr, respectively. The median values of dilatation in the regions of shear and extension are 19 and 45.3 nstrain/yr, respectively. Dilatation in the region of extension is significantly greater than that in the region of shear (at α = 0.001). Average and median values of dilatation in the region of compression are only −5 and −3 nstrain/yr, respectively and are statistically less than dilatation in the regions of shear and extension. However, dilatational strain is negative only in seismic zones 23 through 25 (average of −26.5 and median of −22.9 nstrain/yr) where plate convergence is transpressional. The average and median values of shear strain in zones 23–25 are 95.5 and 103.4 nstrain/yr, respectively. In seismic zones 20–22, plate movements are transtensional: the dilatation is positive with average value of 16.4 nstrain/yr and median value of 18.3 nstrain/yr. The shear strain in zones 20 through 22 has average and median values of 72.7 and 68.9 nstrain/yr, respectively).

[32] Significant correlation between b value and GPS strain is limited to that observed in the region of compression. As mentioned earlier, in this region, the shear strain correlates negatively with b value (−0.83, p = 0.04). The correlation of dilatation to b value is weakly positive (r = 0.73 with p = 0.1). The correlation coefficient increases to 0.97 when we look only at the three observations from seismic zones 23–25 where dilatation is negative; however the probability that the slope of the regression line could actually be zero increases to 0.15. These three observations are too few to make a more definitive conclusion. However, in either case, the relationship suggests the tendency to have increasingly negative dilatation with smaller b value; i.e., increased compressive deformation leads to increased probability of higher-magnitude seismicity. The absence of greater significance in the correlation between b and dilatation in the region of compression is most likely related to the variability in plate interaction from transtensional in the east (zones 20–22) to transpressional in the west (zones 23–25).

[33] The relationship of seismicity distribution (D) to b value and strain is well defined only in the region of shear (the NAFZ). In the region of shear, D correlates with b at regional scale (full range and 10 to 40 km scales).

5. Discussion and Conclusions

5.1. Fractal Range and Heterogeneity

[34] Analysis reveals significant variation in the multifractal properties of seismicity between the tectonic subdivisions of the area (see Table 2). For example, D_2 (full range) along the subduction zone has median value of 1.64 and is statistically different from median D_2 in the regions of shear and tension (1.43 and 1.41, respectively) at the α = 0.05 level. Median values of D_{15} are less than D_2 in all cases, but significant differences between the values of D_{15} in the different tectonic subdivisions do not

occur. The differences in D_2 suggest that regions deformed by shear and extension are generally characterized by more clustered patterns of seismicity than in areas deformed by compression. However, the higher threshold magnitude used in the region of compression may be responsible for the more diffuse nature of seismicity observed there.

[35] The time span is held constant throughout this study. In addition, the range of r for which D is computed is also held constant. This ensures that the results are reproducible and that variations in the parameters are not simply the result of differences in time interval or spatial range over which the estimates are made. This allows us to interpret our results in terms of the seismotectonic attributes of distinct regional tectonic subdivisions.

5.2. The b Value and GPS Deformation Rate

[36] The median b value observed along the NAFZ (strike-slip zone) is 1.24; this is almost identical to the median b value associated with shallow thrusting in the region of compression (1.23). However, the GPS strain data suggests the region of compression could actually be subdivided into two segments: one of transtension (zones 20–22) and the other, transpression (zones 23–25). The median b values in these two subdivisions are 1.44 and 1.21 respectively. Median b value in the transtensional segment of this region is larger than that in the region of extension (1.34) and suggests lower likelihood of larger magnitude seismicity along this segment of the subduction zone.

[37] Significant correlation of D_2 and D_{15} to GPS strain is limited to that observed over the 10 to 40 km scale in the region of extension with dilatation strain. The correlation between D_2 and dilatation is 0.67 ($p = 0.02$) and between D_{15} and dilatation, 0.73 ($p = 0.01$). The correlation of b to GPS strain is limited to that observed in the region of compression. There, b correlates negatively with shear ($r = -0.83$, $p = 0.04$) and has marginally significant positive correlation to dilatation ($r = 0.73$, $p = 0.1$). The relation between shear strain and dilatation is significant only along the NAFZ (-0.79, $p = 0.03$).

5.3. Correlation and Seismic Hazard

[38] The results obtained from analysis of data along the NAFZ suggest that as the probability of larger magnitude earthquakes becomes smaller (larger b value) the epicenter distribution becomes less clustered (higher D). Significant relationships between D and b in the regions of extension and compression are not observed. The relationship is unique to the strike-slip zone. The positive relationship between D and b observed along the NAFZ may be an indicator of increased seismic hazard, consistent with the theoretical results of *Main* [1992]. *Öncel and Wilson* [2002] tentatively proposed the idea based on changes observed along the western segment of the NAFZ. In that study, changes in b and D were followed during the period of time extending from 1945 through 1988. In their study they show that the correlation between D and b changes from -0.92 (1945 to 1975) to 0.48 (1976 to 1988). The current analysis conducted over the 1981 through 1998 time period reveals that this positive correlation continued to increase (0.81 and 0.75 for D_2 and D_{15}, respectively) in the years leading up to the Izmit earthquake. The relationship reflects a tendency to have increased levels of low-magnitude seismicity develop on a widely scattered distribution of epicenters. The general trend of westward migrating seismicity during the 1900 to 1990 time period, the recent large slip rates occurring in the central NAFZ, and the lower slip rates in the western NAFZ suggest that stress has been focused into the western NAFZ. *Öncel and Wilson* [2002] note that the anomalous changes between b and D_C observed during the 1976–1988 time frame along the western segment of the NAFZ may have been a warning sign that increased levels of low-magnitude seismicity did not effectively release stress accumulation. The analysis conducted here shows the presence of an even stronger positive correlation in the years leading up to the Izmit earthquake. Additional analysis of the temporal variations between D and b over the recent 1999 to 2004 following the Izmit earthquake may help to establish the significance of this relationship as a hazard indicator.

[39] Seismotectonic parameters D_q (D_2 and D_{15}) and the Gutenberg-Richter b value have limited correlation to GPS-derived strain in the western Turkey study area. This area contains regions being deformed predominantly in response to strike slip, extension, and subduction. Multifractal measures of epicenter distribution (D_2 and D_{15}) suggest that the patterns of seismicity are more clustered in the regions deformed predominantly by shear and extension than along the Aegean subduction zone. Significant correlation of b value to GPS-derived strains occurs only in the region of compression (Aegean subduction zone). There, b correlates negatively with shear and shows a tendency to positive correlation with dilatation. These relationships suggest that in this area, shear and dilatation strain rates can be used to predict the probability of larger magnitude earthquakes. This relationship is consistent with our expectations that decreases of b will accompany increased shear and increasingly negative dilatation (or compressive strain).

[40] Along the NAFZ (region of shear) a significant positive correlation exists between seismic clustering (D) and the Gutenberg-Richter b value that is largely associated with patterns of regional-scale seismicity. No correlation was observed between b and GPS strain in this region. *Öncel and Wilson* [2002] noted that a transition from negative to positive correlation between D and b value along the NAFZ occurred during the 1975 to 1988 time period. Analysis presented in this paper reveals an even stronger positive correlation during the 1981 to 1998 time period preceding the 1999 Izmit earthquake.

[41] **Acknowledgments.** We thank Xinglin Lei (Geological Survey of Japan) for providing the multifractal analysis software and his guidance in the use of his program. This study was supported in part through AIST supported Visiting Fellowship with the Geological Survey of Japan (Öncel). We are grateful to Abhey Bansal, an anonymous referee, Allison Bent, Maurice Lamontagne and John Adams for their review. Figure 1 was prepared from data available from the Geoscience Interactive Databases (version 1.0c), Cornell University/INSTOC.

References

Aki, K. (1965), Maximum likelihood estimate of b in the formula log N = a – bM and its confidence limits, *Bull. Earthquake Res. Inst. Tokyo Univ.*, *43*, 237–239.

Davis, J. C. (2002), *Statistics and Data Analysis in Geology*, John Wiley, Hoboken, N.J.

Dewey, J. F., W. C. Pitman, W. B. F. Ryan, and J. Bonnin (1973), Plate tectonics and the evolution of the Alpine system, *Geol. Soc. Am. Bull.*, *84*(84), 3137–3180.

Eyidogan, H. (1988), Rates of crustal deformation in western Turkey as deduced from major earthquakes, *Tectonophysics*, *148*, 83–92.

Godano, C., and V. Caruso (1995), Multifractal analysis of earthquake catalogs, *Geophys. J. Int.*, *121*, 385–392.

Grassberger, P., and I. Procaccia (1983), Measuring the strangeness of strange attractors, *Physica D*, *9*, 189–208.

Gutenberg, B., and C. F. Richter (1954), *Seismicity of the Earth and Associated Phenomena*, Princeton Univ. Press, Princeton, N. J.

Havstad, J. W., and C. L. Ehlers (1989), Attractor dimension of non-stationary dynamical systems from small data sets, *Phys. Rev. A*, *39*, 845–853.

Hentschel, H. G. E., and I. Procaccia (1983), The infinite numbers of generalized dimensions of fractals and strange attractors, *Physica D*, *8*, 435–444.

Hirabayashi, T., K. Ito, and T. Yoshi (1992), Multifractal analysis of earthquakes, *Pure Appl. Geophys.*, *138*(4), 591–610.

Kagan, Y. Y. (1994), Observational evidence for earthquakes as a nonlinear dynamic process, *Physica D*, *77*, 160–192.

Kagan, Y. Y., and D. D. Jackson (1991), Long-term earthquake clustering, *Geophys. J. Int.*, *104*, 117–133.

Kahle, H. G., C. Straub, R. Reilinger, S. McClusky, R. King, K. Hurst, G. Veis, K. Kastens, and P. Cross (1998), The strain rate field in the eastern Mediterranean region, estimated by repeated GPS measurements, *Tectonophysics*, *294*, 237–252.

Kahle, H. G., R. Cocard, Y. Peter, A. Geiger, R. Reilinger, S. McClusky, R. King, A. Barka, and G. Veis (1999), The GPS strain rate field in the Aegean Sea and western Anatolia, *Geophys. Res. Lett.*, *26*(16), 2513–2516.

Kahle, H. G., M. Cocard, Y. Peter, A. Geiger, R. Reilinger, A. Barka, and G. Veis (2000), GPS-derived strain rate field within the boundary zones of the Eurasian, African, and Arabian plates, *J. Geophys. Res.*, *105*(B10), 23,353–23,370.

Kiratzi, A. A. (2002), Stress tensor inversions along the westernmost North Anatolian Fault Zone and its continuation into the North Aegean Sea, *Geophys. J. Int.*, *151*, 360–376.

Lei, X. L., K. Kusunose, T. Satoh, and O. Nishizawa (2003), The hierarchical rupture process of a fault: An experimental study, *Phys. Earth Planet. Inter.*, *137*(1–4), 213–228.

Main, I. (1992), Damage mechanics with long-range interactions: Correlation between the seismic b-value and the fractal two-point correlation dimension, *Geophys. J. Int.*, *111*, 531–541.

Main, I. (1996), Statistical physics, seismogenesis, and seismic hazard, *Rev. Geophys.*, *34*(4), 433–462.

Main, I. (2000), Apparent breaks in scaling in the earthquake cumulative frequency-magnitude distribution: Fact or artifact?, *Bull. Seismol. Soc. Am.*, *90*(1), 86–97.

Main, I., and P. W. Burton (1989), Seismotectonics and the earthquake frequency-magnitude distribution in the Aegean area, *Geophys. J. Int.*, *98*, 575–586.

Nakaya, S., and T. Hashimoto (2002), Temporal variation of multifractal properties of seismicity in the region affected by the mainshock of the October 6, 2000 western Tottori Prefecture, Japan, earthquake ($M = 7.3$), *Geophys. Res. Lett.*, *29*(10), 1495, doi:10.1029/2001GL014216.

Öncel, A. O., and T. H. Wilson (2002), Space-time correlations of seismotectonic parameters: Examples from Japan and from Turkey preceding the Izmit earthquake, *Bull. Seismol. Soc. Am.*, *92*(1), 339–349.

Öncel, A. O., and T. H. Wilson (2003), Space-time correlations of seismotectonic parameters: Examples from Japan and from Turkey preceding the Izmit earthquake, paper presented at International Work Shop on North Anatolian, East Anatolian and Dead Sea Fault Systems, Geol. Surv. of Jpn., Ankara, Turkey.

Öncel, A. O., Ö. Alptekin, and I. Main (1995), Temporal variations of the fractal properties of seismicity in the western part of the north Anatolian fault zone: Possible artifacts due to improvements in station coverage, *Nonlinear Processes Geophys.*, *2*, 147–157.

Öncel, A. O., I. Main, O. Alptekin, and P. Cowie (1996a), Spatial variations of the fractal properties of seismicity in the Anatolian fault zones, *Tectonophysics*, *257*, 189–202.

Öncel, A. O., I. Main, O. Alptekin, and P. Cowie (1996b), Temporal variations in the fractal properties of seismicity in the North Anatolian Fault Zone between 31°E and 41°E, *Pure Appl. Geophys.*, *147*(1), 147–159.

Öncel, A. O., T. H. Wilson, and O. Nishizawa (2001), Size scaling relationships in the active fault networks of Japan and their correlation with Gutenberg-Richter b values, *J. Geophys. Res.*, *106*(B10), 21,827–21,841.

Pacheco, J. F., C. H. Scholz, and L. R. Sykes (1992), Changes in the frequency-size relationship from small to large earthquakes, *Nature*, *355*, 71–73.

Papazachos, B. P., and A. A. Kiratzi (1996), A detailed study of the active crustal deformation in the Aegean and surrounding area, *Tectonophysics*, *253*, 129–153.

Smith, A. G. (1976), Plate tectonics and orogeny: A review, *Tectonophysics*, *33*, 215–285.

Sunmonu, L. A., V. P. Dimri, M. R. Prakash, and A. R. Bansal (2001), Multifractal approach to the time series of M >= 7. 0 earthquake in Himalayan region and its vicinity during 1895–1995, *J. Geol. Soc. India*, *58*(2), 163–169.

Taymaz, T., J. Jackson, and D. Mckenzie (1991), Active tectonics of the north and central Aegean Sea, *Geophys. J. Int.*, *106*, 433–490.

Ucer, S. B., S. Crampin, R. Evans, A. Miller, and N. Kafadar (1985), The Marnet radiolinked seismometer network spanning the Marmara Sea and the seismicity of western Turkey, *Geophys. J. R. Astron. Soc.*, *83*(1), 17–30.

Wiemer, S., and M. Wyss (2000), Minimum magnitude of completeness in earthquake catalogs: Examples from Alaska, the western United States, and Japan, *Bull. Seismol. Soc. Am.*, *90*(4), 859–869.

Wilson, T. H. (2001), Scale transitions in fracture and active fault networks, *Math. Geol.*, *33*, 591–613.

A. O. Öncel, Active Fault Research Center, Geological Survey of Japan, Site 7, Higashi, 1-1, Tsukuba, Ibaraki 305-8567, Japan. (oncel@hotmail.com)

T. Wilson, Department of Geology and Geography, West Virginia University, Morgantown, WV 26506-6300, USA.